Chapter 2
Adaptive Sampling with a Fleet of Autonomous Sailing Boats Using Artificial Potential Fields

Hadi Saoud, Frédéric Plumet and Faiz Ben Amar

Abstract Autonomous sailing boats are an attractive solution to perform measurements at sea thanks to their low energy consumption. A fleet of such vehicles can also be used for adaptive sampling of an environmental field. In previous work, artificial potential fields have been used successfully in a local and real-time planner to carry out the autonomous navigation of one sailing boat. In this paper, we first extend the previous method to include marine current in the local planning and show how this extension can improve the safety and navigation performances in the case of strong marine current. Next we show how the same planning method can be used to control a formation of sailboats and perform adaptive sampling of some natural quantities and can be easily tuned to exhibit different behaviors such that way-point reaching, gradient or isoline following.

2.1 Introduction

Oceans observation at mesoscale (10–100 km) or sub-mesoscale (1–10 km) is an important issue for researcher in order to better understand how the marine environment evolves. However, at these scales, satellite remote sensing provides neither enough details on the sea surface nor provides information on the water column structure and these observation must be complemented by measures carried out by drifting profilers, research vessels, moored or drifting buoys for examples. Moreover, in marine environment, physical, chemical or biological fields have usually

H. Saoud · F. Plumet (✉) · F. Ben Amar
Sorbonne Universités, UMR 7222, ISIR, UPMC Univ Paris 06, 75005 Paris, France
e-mail: plumet@isir.upmc.fr

H. Saoud
e-mail: saoud@isir.upmc.fr

F. Ben Amar
e-mail: amar@isir.upmc.fr

F. Plumet
Université Versailles St-Quentin, UMR 7222, ISIR, 75005 Paris, France

L. Jaulin et al. (eds.), *Marine Robotics and Applications*, Ocean Engineering & Oceanography 10, https://doi.org/10.1007/978-3-319-70724-2_2

high spatio-temporal variability. It is so often desirable to perform adaptive sampling of these quantities at a scale compatible with the observed structure [2].

With the development of smaller and lower cost sensors, new solutions using autonomous robots (surface or underwater) begin to emerge in order to carry these sensors where measurements are more likely to be useful [8, 15, 18, 19, 27]. Using such low cost vehicles, adaptive sampling can thus be performed by following the gradient of some physical, chemical or biological parameter. To perform such gradient-based navigation in an efficient way (time constraints), a fleet of vehicles is usually required, even if it remains possible using a single vehicle (see [3] for example). Examples of gradient following navigation for a fleet of vehicles can be found in [1, 9, 14, 20].

Focusing on Autonomous Surface Vehicles (ASV), numerous robots have been developed for bathymetric data recording in shallow water [16], monitoring of various marine environmental data either alone [4, 17, 26] or as part of a sensor network [6, 7, 21, 24]. However, all of these aforementioned vehicles are conventional electrically powered systems and suffer from a lack of autonomy that restrains their usage to short-term missions. Autonomous sailing robots could then be an efficient solution for mesoscale oceans observation since they rely on renewable energy such as solar and wind energies [5, 25].

However, the control of autonomous sailboats is faced with two inherent difficulties: the uncontrollable and partially unpredictable nature of thrust forces (wind direction and wind speed) on one hand and the complex kinematics of a sailboat (aero and hydrodynamic properties of sails and hull) on the other hand. In previous work, we used artificial potential fields method [12, 13] in a local path planning algorithm that address these two problems simultaneously. This navigation method is able to react in real-time to changes in the environment and control the vehicle towards a given waypoint [22].

In this paper, we use the same framework of artificial potential field for gradient climbing of a natural field using a formation of autonomous sailboats. For the sake of clarity, the method used to control the motion of one single sailboat is first presented in Sect. 2.2. Since we focus on oceans parameters measurements, it is also necessary to consider the existence of ocean currents. Obviously, if strong current exists, the sailboat will drift and may not be able to reach it's final destination. Section 2.3 shows how to address these currents in the local path planning algorithm and how this extension can enhance the performance and safety of navigation in the case of strong marine currents. We made the assumption that these currents are known either through a marine chart or by local measurements made by the sailboat. Section 2.4 presents how adaptive sampling of a given natural field by a formation of autonomous sailboats easily fits in the general framework of potential field planning. The proposed method is based on the definition of a reference formation. The motion of the reference formation as well as the motion of the real vehicles are controlled by a local potential field planner i.e. each real vehicle is attracted by a potential field attached to the corresponding reference vehicle in the reference formation. The assumption is made

that there exists a bidirectional communication link between the different vehicles to share the current and desired positions of the real vehicles as well as the position of the reference formation. Simulation results are presented and shows that this method can easily be tuned to exhibit different behavior such that way-point reaching for an entire formation, gradient or isoline following of a natural potential field.

2.2 Potential Field Planning of One Single Sailboat

Potential field (PF) method can be an efficient way to achieve local path planning for mobile robots. Since this method is a local one, its main drawback is that the moving vehicle may fall into a local minimum when the obstacle density is high. Luckily, open sea rarely have a high density of obstacles, making the potential field method a very convenient path planning algorithm for autonomous sailboats [10, 11, 23].

The fact that this method is local is also an advantage because the computational burden remains the same even if the obstacles or the goal are moving. This property was used to design a local planner for an autonomous sailboat, with the kinematic constraints of the sailboat transformed in obstacles moving with the vehicle. This property will also be used to design the local path planning algorithm for a formation of sailboat, with a moving goal (attractive potential) attached to each node of the reference formation (see Sect. 2.4).

In potential field based planning method, the vehicle has to follow the direction defined by the gradient of a scalar field. For autonomous sailboat path planning, the field is the summation (see Fig. 2.1) of several exo-potential fields and an endo-potential field:

- exo-potential fields are repulsive potentials centered at each obstacles position and an attractive field centered at the goal position,
- endo-potential field is a repulsive potential, moving with the sailboat and depending on the actual wind condition, that reflects the sailboat kinematics.

In practice, the gradient is evaluated numerically on a vehicle-centered ring at each sample time, using the actual value of the wind (speed and direction) measured by the sailboat and the position of a given way-point. Thus, at each time instant, the minimum of the local gradient defines the desired heading of the sailboat.

Notice that, since the desired heading is defined by the weighted sum of several potentials, the attractive potential must be defined as $U_g = K_g\, d_{goal}$ to guarantee that the sailboat will not tack too frequently or go into a no-go zone when the distance to the goal d_{goal} is important.

The endo-potential is built on the basis of the speed polar diagram of the sailboat (see Fig. 2.2). For a given wind speed, this polar curve shows the boat speed (in steady state) as a function of the angle γ between the heading and the true wind vector. Two high repulsive potentials are used to represent the upwind and downwind no go-zones.

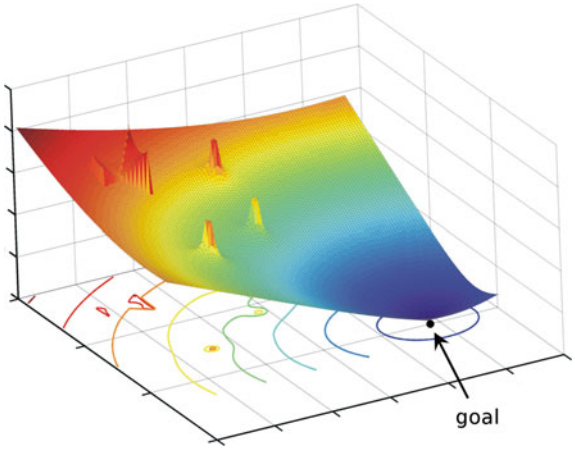

Fig. 2.1 Overall potential relative to three obstacles and a goal point (waypoint)

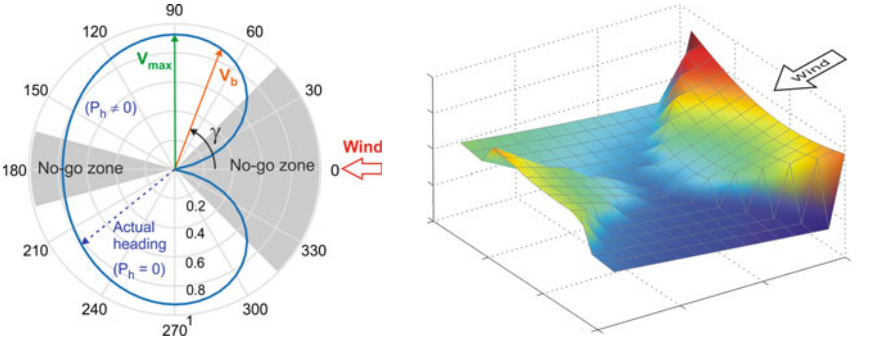

(a) Speed polar diagram of a sailboat (b) Close view of the endo-potential around the boat

Fig. 2.2 Endo-potential around the boat based on the speed polar diagram

Another potential P_w is added to reflect the speed performances of the sailboat. This potential can be defined as:

$$P_w = G_w \frac{V_{Max} - V_b}{V_{Max}} + P_h$$

with V_b the boat speed, V_{Max} the maximum boat speed and G_w a given weighting factor. In order to take the cost of gybing and tacking into account, an hysteresis potential $P_h \neq 0$ is added for the navigation area on the other side of the wind, relative to the actual heading.

2.3 Including Marine Currents

For application such that oceans parameters measurements with sailboats, it can be also mandatory to take ocean currents into account. Obviously, in such a case, the sailboat will drift and may not be able to reach it's final destination if the current is strong enough. We assume here that these ocean currents are known either through a marine chart or by local measurements made by the sailboat.

Since the local path planning algorithm is based on the speed polar diagram, we can easily include the marine currents by modifying the speed polar diagram.

Let $\vec{V}_b^{\mathcal{I}}$ be the boat velocity vector in the inertial frame $\mathcal{I}$, $\vec{V}_b^{\mathcal{C}}$ the boat velocity with respect to the current frame $\mathcal{C}$ and $\vec{V}_c^{\mathcal{I}}$ the current velocity with respect to the inertial frame $\mathcal{I}$. Using the same notation for the wind vector, we can write:

$$\vec{V}_b^{\mathcal{I}} = \vec{V}_b^{\mathcal{C}} + \vec{V}_c^{\mathcal{I}} \quad \text{and} \quad \vec{V}_w^{\mathcal{I}} = \vec{V}_w^{\mathcal{C}} + \vec{V}_c^{\mathcal{I}}$$

Assuming that, for a given wind speed, the boat velocity vector $\vec{V}_b$ is given by a polar function $P()$ depending on the true wind vector $\vec{V}_w$ and angle γ between these two vectors (see Fig. 2.2a):

$$\vec{V}_b = P\left(\vec{V}_w, \gamma\right)$$

This relationship remains the same if both velocity vectors are expressed in the same frame. Since:

$$\vec{V}_b^{\mathcal{C}} = P\left(\vec{V}_w^{\mathcal{C}}, \gamma\right)$$

the boat velocity in the inertial frame is given by:

$$\vec{V}_b^{\mathcal{I}} = \vec{V}_b^{\mathcal{C}} + \vec{V}_c^{\mathcal{I}} = P\left(\vec{V}_w^{\mathcal{I}} - \vec{V}_c^{\mathcal{I}}, \gamma\right) + \vec{V}_c^{\mathcal{I}} \tag{2.1}$$

The resulting speed polar diagram (taking into account the effect of the marine current) is then the result of a translation (due to the $\vec{V}_c$ vector) and a slight deformation due to the non-linear effect of the $P()$ function. This is illustrated Fig. 2.3 for $\vec{V}_w^{\mathcal{I}} = [-2, 0]^t\ (m/s)$ and $\vec{V}_c^{\mathcal{I}} = [-0.25, 0.25]^t\ (m/s)$.

This modified speed polar diagram can then be used to build the adapted endo-potential around the sailboat. An example, showing the results of a local path planning, is depicted Fig. 2.4 using either the conventional speed polar polar diagram (see Fig. 2.4a) or the adapted version to take currents into account (Fig. 2.4b). For these simulations, the wind speed is equal to 4 m/s, the current speed is equal to 0.5 m/s and their directions are depicted Fig. 2.4.

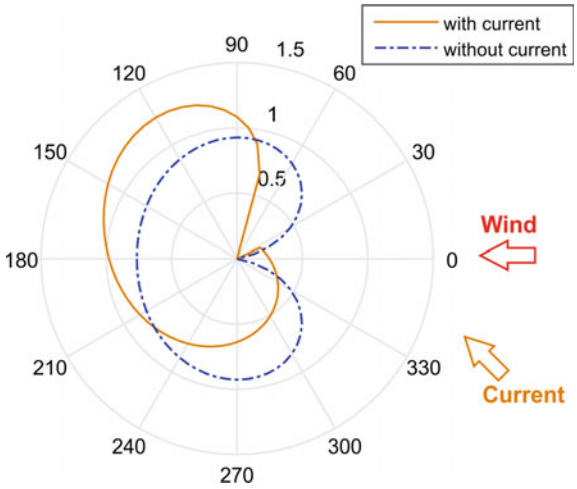

Fig. 2.3 Speed polar diagram with marine current ($\overrightarrow{V}_w^{\mathcal{I}} = [-2, 0]^t$ and $\overrightarrow{V}_c^{\mathcal{I}} = [-0.25, 0.25]^t$)

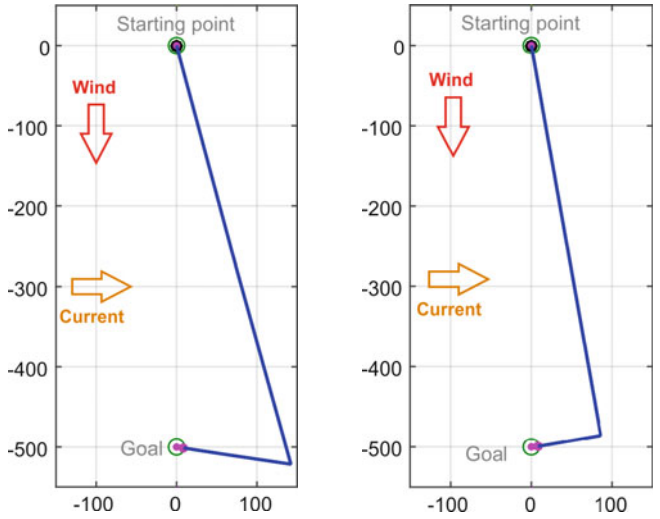

(a) Resulting path, without taking current into account

(b) Resulting path, taking current into account

Fig. 2.4 Potential field based planning with and without taking into account oceans current

One can see that, when taking currents into account in the path planning algorithm, the boat follows a more direct route toward the goal. Moreover, the time to reach the waypoint is equal to 9.1 mn when taking currents into account and equal to 10.8 mn when using the conventional method, which corresponds to an enhancement of more than 10% to the total traveling time.

2.4 Formation Control

As mentioned before, the general framework of potential field based planning can easily be adapted to solve the problem of gradient following of a natural field with a fleet of sailboats. Moreover, since potential field algorithm is a local path planning method, the computational burden remains the same if the goal is moving. This property will be used to control a formation of sailboats.

The basic idea is to define first a reference formation where each node of the reference formation becomes an attractive goal for one corresponding real sailboat. Then, the whole reference formation is steered toward a given waypoint or driven to follow the gradient of a natural potential field. In this way, the vehicles remains in formation but can adapt their motion to the local wind conditions.

We first define the reference formation as a rigid lattice, with each node of the lattice corresponding to a reference (virtual) vehicle. Let ${}^{(i)}S_{Ref}$ be the position of the (i) reference vehicle and R a local frame attached to the reference formation. Without loss of generality, we assume here a triangular formation with a local frame R attached to the first node of the formation (see Fig. 2.5a).

The motion of each real sailboat (i) is then driven by a force ${}^{(i)}\vec{F}$ coming from the overall potential ${}^{(i)}U$:

$$ {}^{(i)}\vec{F} = \overrightarrow{grad}\left({}^{(i)}U\right) = {}^{(i)}\vec{F}_g + {}^{(i)}\vec{F}_o + {}^{(i)}\vec{F}_w \tag{2.2} $$

with ${}^{(i)}\vec{F}_g$ the attractive force coming from the (i) reference vehicle, ${}^{(i)}\vec{F}_o$ the force due to external obstacles as well as other real vehicles and ${}^{(i)}\vec{F}_w$ the force coming from the endo-potential of the speed polar diagram, including marine currents if present. This way, each real sailboat is linked to a moving reference node in the reference formation (see Fig. 2.5b) but remains free to locally adapt its motion to varying wind and current conditions as well as avoiding collision with other vehicles of the formation (or external obstacles). These forces, as well as the positions of the

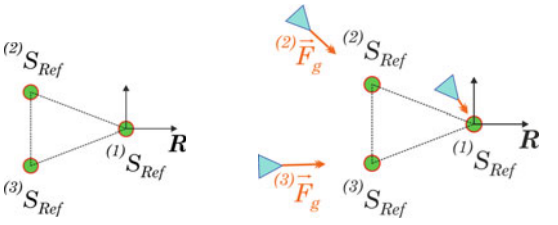

Fig. 2.5 Definition of the reference formation with the corresponding real vehicles

(a) Reference formation, with its attached frame R

(b) Reference formation with the "linked" real vehicles

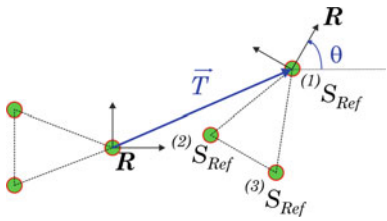

Fig. 2.6 Displacement of the reference formation

reference nodes are computed at each sampling time T_s of the local path planning algorithms implemented on each vehicle.

The last step is the displacement of the whole reference formation. This displacement is defined by a translation $\vec{T}$ and a rotation θ of frame R with respect to the previous position of the frame (see Fig. 2.6).

- The norm of the translation vector can be used to perform a cruise control of the whole formation and ensures that each vehicle remains in the vicinity of its corresponding reference node and can be computed, for example, as:

$$\left|\vec{T}\right| = Max\left(V_d T_s - K_v\,\overline{dist}, 0\right)$$

  with V_d the desired velocity of the reference formation, $\overline{dist}$ the mean distance between the sailboats and their corresponding reference positions and K_v a positive scalar.

The direction of this vector is chosen accordingly to the mission objective: reach a waypoint, follow the gradient or an isoline of a natural field (computed locally by the fleet of sailboats). This direction can be computed either directly (for gradient or isoline following tasks for example) or by using a potential field path planning algorithm to drive the whole reference formation toward a feasible direction (for waypoint reaching for example).

- The orientation θ can be set arbitrarily.
  For example:
  - if $\theta = 0$, the orientation of the reference formation remains constant with respect to a given fixed frame,
  - if θ is chosen such that $\overrightarrow{{}^{(2)}S_{Ref}\ {}^{(3)}S_{Ref}}$ remains perpendicular to $\vec{T}$, the formation is pointing toward the goal with the first reference vehicle becoming the leader of the formation.

In order to test this formation control algorithm under varying wind angle and wind speed, a simulation environment has been designed. This environment is defined by a constant (mean) value of wind speed and wind angle as well as weather disturbance areas with a Gaussian distribution around a maximum value (see Fig. 2.7 for an example).

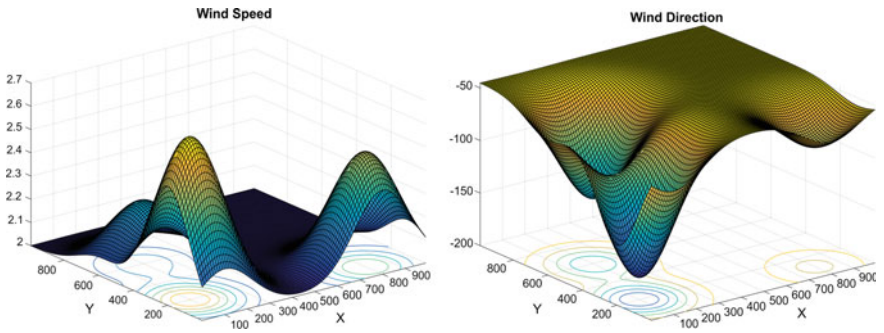

(a) Wind speed (b) Wind angle

Fig. 2.7 Wind field in the area

In the following simulations, the marine current was supposed to be null and the following simplified kinematic model of the sailboat was used:

$$\begin{cases} \dot{x} = u\ \cos(\psi) \\ \dot{y} = u\ \sin(\psi) \\ u = \left|\vec{V}_b\right| = \left|P(\vec{V}_w, \psi - \phi)\right| \end{cases}$$

with ψ the boat heading (defined by PF algorithm) and ϕ the wind angle.

Figure 2.8 shows the simulation result of a mission consisting in reaching a waypoint on $[300, 400]\,m$, starting from $[100, 100]\,m$. In this case, the fleet is constrained to stay in a leader-follower formation (for the reference formation, θ is chosen such that $\overrightarrow{{}^{(2)}S_{Ref}\ {}^{(3)}S_{Ref}}$ remains perpendicular to $\vec{T}$) and the PF planning is applied to the leader of the reference formation (origin of the moving frame R). One can notice that the formation leader (as well as its "linked" real sailboat) is going directly to the goal while the second vehicle has to perform maneuvers (tacking) due to the local wind conditions in order to reach the waypoint.

The same control algorithm can be used for adaptive sampling of a natural parameter. In this case, each sailboat is supposed to be able to measure the given parameter and the hypothesis is also made that, given these measurements at each sample time, a representative gradient of the field can be estimated. The previous method can be readily used in this case except that a PF planning algorithm is no more used in order to compute the direction of motion of the reference formation (direction defined by the $\vec{T}$ vector). Instead, the gradient of the natural field is directly used to define the direction of $\vec{T}$.

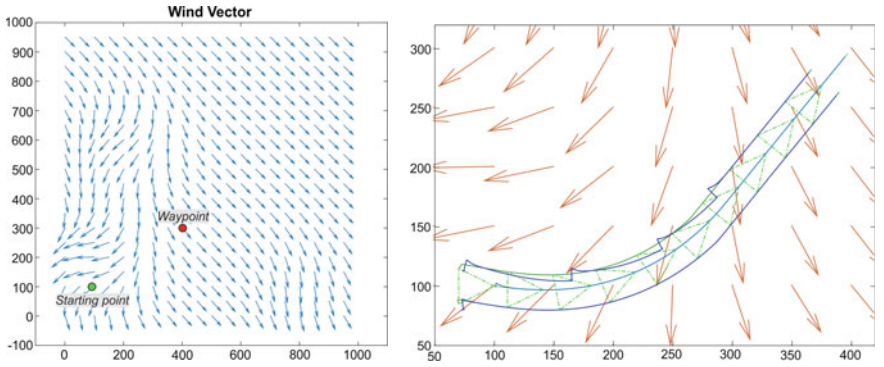

(a) Wind vector (b) Sailboats trajectories and local wind vector

Fig. 2.8 Waypoint reaching: sailboats and reference formation trajectories

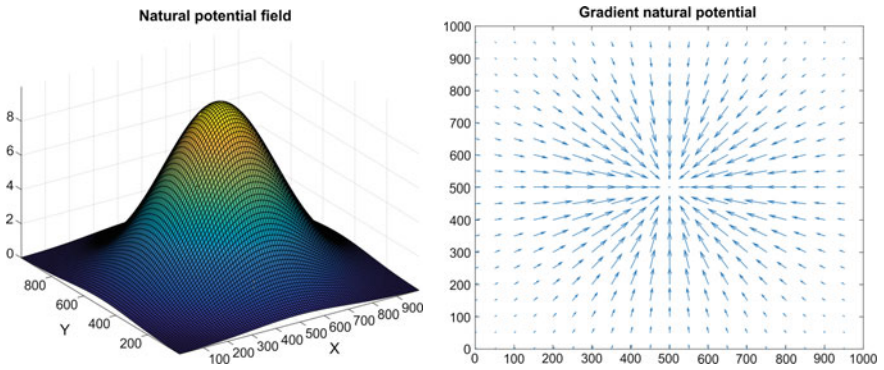

(a) Natural field (b) Gradient of the natural field

Fig. 2.9 Natural field and gradient of this field

Figure 2.9 shows an example of a natural field build on the basis of a Gaussian distribution around a central point located at the center of the map.

The mission depicted Fig. 2.10 consists of following the gradient of the natural field and then, when a given value of the field is reached, following the isoline contour of the field. One can notice that the sailboats are first moving upwind with several tacking maneuvers when following the gradient then follow a contour line at a constant value of the natural field (gradient of the natural field are depicted by arrows on Fig. 2.10b). In this case, we chose a constant orientation in a fixed frame for the reference formation ($\theta = 0$).

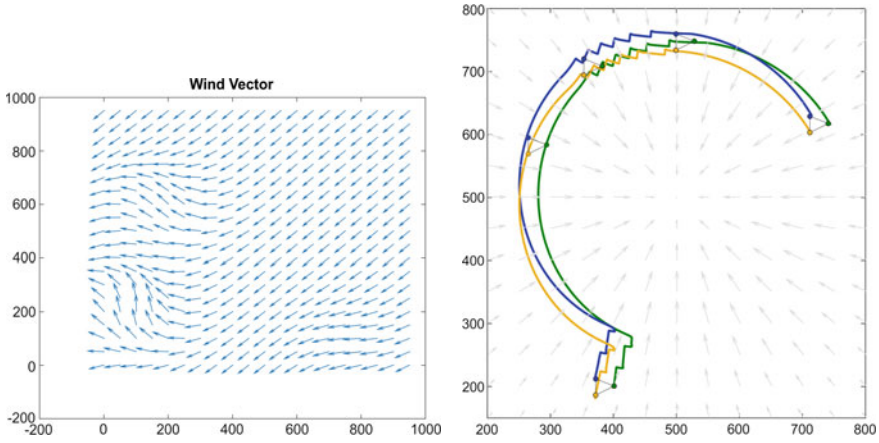

(a) Wind vector

(b) Sailboats trajectories and gradient of the natural field

Fig. 2.10 Gradient then isoline following: wind vector and sailboats trajectories

2.5 Conclusion

This paper proposed a potential field planning method to control a formation of sailboats that can be used to perform adaptive sampling of a given natural parameter. The method is based on the definition of a rigid reference formation, with each sailboat linked to a node of this reference formation through an attractive potential. The effect of marine currents can be taken into account by modifying the speed polar diagram of the sailboat, which forms the core of the local planning algorithm. Several simulations show the effectiveness of the method for missions such that waypoint reaching, gradient or isoline following of a natural field under spatially varying wind conditions. This method can easily be implemented in real time on small embedded computer, provided that a bidirectional communication link exists between the sailboats for the coordinated motion control and exchange of local measurements of the natural parameter to build a local estimation of the natural field gradient.

References

1. T. Adamek, C.A. Kitts, I. Mas, Gradient-based cluster space navigation for autonomous surface vessels. IEEE/ASME Trans. Mech. **20**(2), 506–518 (2015)
2. A. Alvarez, B. Garau, A. Caiti, Combining networks of drifting profiling floats and gliders for adaptive sampling of the ocean, in *IEEE International Conference on Robotics and Automation* (2007), pp. 157–162

3. E. Burian, D. Yoerger, A. Bradley, H. Singh, Gradient search with autonomous underwater vehicles using scalar measurements, in *Symposium on Autonomous Underwater Vehicle Technology* (1996), pp. 86–98
4. M. Caccia, R. Bono, G. Bruzzone, E. Spirandelli, G. Veruggio, A.M. Stortini, G. Capodaglio, Sampling sea surfaces with SESAMO: an autonomous craft for the study of sea-air interactions. IEEE Robot. Autom. Mag. **12**(3), 95–105 (2005)
5. N.A. Cruz, J.C. Alves, Autonomous sailboats: an emerging technology for ocean sampling and surveillance, in *MTS/IEEE OCEANS* (2008)
6. J. Curcio, J. Leonard, A. Patrikalakis, SCOUT-a low cost autonomous surface platform for research in cooperative autonomy, in *MTS/IEEE OCEANS*, vol. 1 (2005), pp. 725–729
7. D.P. Eickstedt, M.R. Benjamin, H. Schmidt, J.J. Leonard, Adaptive control of heterogeneous marine sensor platforms in an autonomous sensor network, in *IEEE/RSJ International Conference on Intelligent Robots and Systems* (2006), pp. 5514–5521
8. C.C. Eriksen, T.J. Osse, R.D. Light, T. Wen, T.W. Lehman, P.L. Sabin, J.W. Ballard, A.M. Chiodi, Seaglider: a long-range autonomous underwater vehicle for oceanographic research. IEEE J. Ocean. Eng. **26**(4), 424–436 (2001)
9. E. Fiorelli, P. Bhatta, N.E. Leonard, I. Shulman. Adaptive sampling using feedback control of an autonomous underwater glider fleet, in *13th International Symposium on Unmanned Untethered Submersible Technology (UUST)* (2003)
10. L. Jaulin, F. Le Bars, A simple controller for line following of sailboats. Int. Robot. Sailing Conf. 117–129
11. L. Jaulin, F. Le Bars, An interval approach for stability analysis: application to sailboat robotics. IEEE Trans. Robot. **29**(1), 282–287 (2013)
12. O. Khatib, Real-time obstacle avoidance for manipulators and mobile robots. Int. J. Robot. Res. **5**(1), 90–98 (1986)
13. B. Krogh, C. Thorpe, Integrated path planning and dynamic steering control for autonomous vehicles. IEEE Int. Conf. Robot. Autom. **3**, 1664–1669 (1986)
14. F. Lekien, L. Mortier, P. Testor, Glider coordinated control and lagrangian coherent structures, in *2nd IFAC Workshop on Navigation, Guidance and Control of Underwater Vehicles* (2008), pp. 125–130
15. N.E. Leonard, D.A. Paley, F. Lekien, R. Sepulchre, D.M. Fratantoni, R.E. Davis, Collective motion, sensor networks, and ocean sampling. Proc. IEEE **95**(1), 48–74 (2007)
16. P. Mahacek, T. Berk, A. Casanova, C. Kitts, W. Kirkwood, G. Wheat, Development and initial testing of a SWATH boat for shallow-water bathymetry, in *MTS/IEEE OCEANS* (2008)
17. P. Mahacek, R. Kobashigawa, A. Schooley, C. Kitts. The WASP: an autonomous surface vessel for the university of alaska, in *MTS/IEEE OCEANS*, vol. 3 (2005), pp. 2282–2291
18. J.E. Manley, Unmanned surface vehicles, 15 years of development, in *MTS/IEEE, OCEANS* (2008), pp. 1–4
19. J.E. Manley, S. Willcox, The Wave Glider: a new concept for deploying ocean instrumentation. IEEE Instrum. Meas. Mag. **13**(6), 8–13 (2010)
20. P. Ogren, E. Fiorelli, N.E. Leonard, Cooperative control of mobile sensor networks:adaptive gradient climbing in a distributed environment. IEEE Trans. Autom. Control **49**(8), 1292–1302 (2004)
21. A. Pascoal, P. Oliveira, C. Silvestre, et al., Robotic ocean vehicles for marine science applications: the european ASIMOV project, in *MTS/IEEE OCEANS 2000*, vol. 1 (2000), pp. 409–415
22. C. Pêtrès, M.A. Romero-Ramirez, F. Plumet, A potential field approach for reactive navigation of autonomous sailboats. Robot. Auton. Syst. **60**(12), 1520–1527 (2012)
23. F. Plumet, C. Petres, M.-A. Romero-Ramirez, B. Gas, Sio-Hoi Ieng, Toward an autonomous sailing boat. IEEE J. Ocean. Eng. **40**(2), 397–407 (2015)
24. G.W. Podnar, J.M. Dolan, A. Elfes, S. Stancliff, E. Lin, J.C. Hosier, T.J. Ames, J. Moisan, T.A. Moisan, J. Higinbotham, E.A. Kulczycki, Operation of robotic science boats using the telesupervised adaptive ocean sensor fleet system, in *IEEE International Conference on Robotics and Automation* (2008), pp. 1061–1068

25. P.F. Rynne, K.D. von Ellenrieder, A wind and solar-powered autonomous surface vehicle for sea surface measurements, in *MTS/IEEE OCEANS* (2008)
26. E.T. Steimle, M.L. Hall, Unmanned surface vehicles as environmental monitoring and assessment tools, in *MTS/IEEE OCEANS* (2006)
27. L. Yongkuan, Auv's trends over the world in the future decade, in *Symposium on Autonomous Underwater Vehicle Technology* (1992), pp. 116–127

http://www.springer.com/978-3-319-70723-5

Marine Robotics and Applications

Jaulin, L.; Caiti, A.; Carreras, M.; Creuze, V.; Plumet, F.;
Zerr, B.; Billon-Coat, A. (Eds.)

2018, VIII, 178 p. 100 illus., 92 illus. in color., Hardcover
ISBN: 978-3-319-70723-5